TWMS J. App. and Eng. Math. V.16, N.8, 2026, pp. 938-952

A NOVEL APPROACH TO THE FIBONACCI NUMBERS BY INVERSE STEREOGRAPHIC PROJECTION

B. ATES[1*], S. ATES[2], A. KUSTEPELI[3], §

Abstract. In this study, a new geometric framework for Fibonacci numbers is introduced through the definition of Fibonacci points, whose components are Fibonacci numbers. These points are then mapped onto the sphere by means of inverse stereographic projection (ISP), providing novel recurrence relations and algebraic structures analogous to those in classical ones. The transformation of Fibonacci-related geometrical entities such as lines and circles is investigated, leading to the definition of new spherical regions associated with Fibonacci parallels and meridians. Furthermore, a deformed version of the Binet–Fibonacci spiral passing through the Fibonacci points is constructed, which may offer applications in modeling biological spiral deviations caused by environmental effects. Classical Fibonacci identities, such as Cassini identities, are revisited in this spherical setting, and their transformations are established. Finally, possible generalizations of these results to higher-dimensional spaces are discussed.

Keywords: Fibonacci Numbers, Stereographic Projection, Spherical Spirals, Deformed Spirals.

AMS Subject Classification: 11B39, 30F45.

1. Introduction

The Fibonacci sequence is a sequence of integers that obeys the recurrence relation:

$$F_n = F_{n-1} + F_{n-2}, \;\; n \geq 2 \;\text{ with }\; F_1 = 1, F_0 = 0, \tag{1}$$

is so fascinating that, despite its simple form, it appears in a wide variety of complex structures in nature, ranging from microscopic organisms to black holes [1], [2]. The

[1] Department of Mathematics, Piri Reis University, Postane, Eflatun Sk. No: 8, 34940, Tuzla, Istanbul, Turkey.
e-mail:bates@pirireis.edu.tr; barisates2002@gmail.com; ORCID: https://orcid.org/0000-0002-8138-7360.
[2] Department of Chemical Engineering, Izmir Institute of Technology Gulbahce Kampusu Urla, Izmir, 35430, Turkey.
e-mail: selcanates3@gmail.com; ORCID: https://orcid.org/0000-0002-0078-0647.
[3] Department of Electrics & Electronics, Izmir Institute of Technology Gulbahce Kampusu Urla, Izmir, 35430, Turkey.
e-mail: alpkustepeli@iyte.edu.tr; ORCID: https://orcid.org/0000-0002-8995-6628.
[*] Corresponding author.
§ Manuscript received: May 17, 2025; accepted: November 03, 2025.
TWMS Journal of Applied and Engineering Mathematics, Vol.16, No.8;

.

arrangement of leaves and phyllotactic spirals in plants such as sunflowers, pine cones, and artichokes can be modeled by Fibonacci numbers, revealing that their growth obeys certain rules [3], [4]. Since the sequence is strongly related to the golden ratio, it also appears in art, architecture, and engineering [5], [6]. The importance of the Fibonacci sequence has led to numerous generalizations into new sequences and polynomials [7]-[9]. In a recent breakthrough work, it was shown that illuminating atoms in a quantum computer with laser pulses arranged in the form of a Fibonacci sequence enables the storage of more information than before [10]. This remarkable result demonstrates that Fibonacci numbers continue to maintain their significance, constantly finding new applications in emerging areas.

Stereographic projection is a conformal mapping from the sphere $\mathbb{S}^2$ to the plane $\mathbb{R}^2$. As illustrated in Fig. 1, the configuration consists of a sphere of radius R centered on the ζ-axis at $C(0,0,R)$ and a plane located just below the sphere at $\zeta = 0$. As shown in Fig. 1, the line connecting the north pole with a point on the sphere intersects the plane at a unique point, which implies that this mapping is one-to-one. Stereographic projection can be applied to both discrete and continuous sets of points. For example, ISP relates lines passing through the origin to circles passing through both the origin and the north pole [11], [12]. This transformation has a wide range of applications in geology [13], differential geometry [14], complex analysis [11], fluid dynamics [15], quantum physics [16], and electromagnetic theory [17], to name just a few.

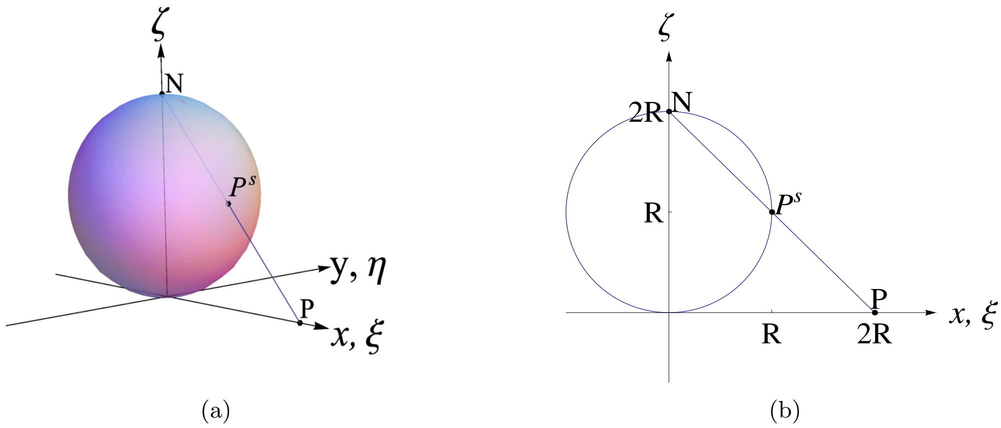

Figure 1. (a) $3D$ illustration of stereographic projection. A line connecting the north pole with an arbitrary point P^s on the sphere intersects the $x-y$ plane at a unique point P. (b) $2D$ view.

In the present work, our aim is to introduce new geometrical representations and relations for Fibonacci numbers. To achieve this, Fibonacci points are defined such that the absolute value of each component of these points is a Fibonacci number. After this initial representation, these points are transformed onto the sphere via inverse stereographic projection (ISP) for the first time. In this way, new algebraic relations are obtained. It is shown that, similar to the well-known recurrence relation of Fibonacci numbers in (1), new recurrence relations on the sphere satisfied by the image points can also be derived. Furthermore, the transformation of Fibonacci-related geometrical objects, such as lines and circles, allows the construction of new configurations on the sphere which enables to describe the regions in terms of Fibonacci numbers through Fibonacci-related parallels and meridians on the sphere's surface. As a realistic application, the deformation of the Binet–Fibonacci spiral passing through the Fibonacci points is considered. This new spiral, while still passing through the Fibonacci points, has a deformed shape. Such a curve could be useful in biology to describe defects in spirals caused by environmental or other external effects. The paper is organized as follows: in Section 2, Fibonacci points on the x-axis are introduced, and their corresponding image points on the sphere are obtained. Using the recurrence relation of Fibonacci numbers in (1), relations among the coordinates of the image points are established. By rotating the Fibonacci points on the x-axis, the transformed form of the recurrence relation is also derived.

To further investigate the relations satisfied by sequential points on the sphere, the well-known Cassini and Fibonacci square type identities and their transformations are considered for special Fibonacci points. Additionally, special lines and circles, both concentric and non-concentric, are examined and their images on the sphere are presented. It is also demonstrated that the parallels and meridians on the sphere can be rearranged and related to Fibonacci numbers. Finally, in Section 3, it is shown that the present results can be directly generalized to higher-dimensional spaces.

2. Inverse Stereographic Projection of a Fibonacci Point

Let us consider a sphere in Cartesian coordinates (ξ, η, ζ) with the following equation

$$\xi^2 + \eta^2 + (\zeta - R)^2 = R^2. \tag{2}$$

As illustrated in Fig.1, a point $P^{\mathrm{s}}(\xi, \eta, \zeta)$ on the sphere is mapped to a unique point $P(x, y)$ on the $x - y$ plane via stereographic projection as

$$P(x, y) \quad = \quad P\left(\frac{2R\xi}{2R - \zeta}, \frac{2R\eta}{2R - \zeta}\right). \tag{3}$$

These equations exhibit the property that the stereographic projection of the north pole $N(0, 0, 2R)$ is not defined [11], [12]. Even though its image is not defined in terms of the stereographic projection, it can be interpreted in connection with the extended complex plane and the Riemann sphere [12]. Conversely, ISP allows one to find the image points $P^{\mathrm{s}}(\xi, \eta, \zeta)$ for a given arbitrary point $P(x, y)$ on the plane, as follows:

$$P^{\mathrm{s}}(\xi, \eta, \zeta) = P^{\mathrm{s}}\left(\frac{4R^2x}{4R^2 + x^2 + y^2}, \frac{4R^2y}{4R^2 + x^2 + y^2}, \frac{2R(x^2 + y^2)}{4R^2 + x^2 + y^2}\right). \tag{4}$$

In the rest of the paper, a point in the $x - y$ plane is called a “Fibonacci point” if the absolute value of each coordinate is a Fibonacci number. Thus, such points can be written in the form

$$P(x, y) = P(c_1F_n, c_2F_m) \tag{5}$$

where c_1 and c_2 are either $+1$ or -1. It is important to note that (3) can be used to check whether the stereographic projection of an arbitrary point on the sphere corresponds to a Fibonacci point or not. The ISP of a Fibonacci point is given by the following relation:

$$P^{\mathrm{s}}(\xi^{\mathrm{F}}_{n,m}, \eta^{\mathrm{F}}_{n,m}, \zeta^{\mathrm{F}}_{n,m}) = P^{\mathrm{s}}\left(\frac{4R^2c_1F_n}{4R^2 + F_n^2 + F_m^2}, \frac{4R^2c_2F_m}{4R^2 + F_n^2 + F_m^2}, \frac{2R(F_n^2 + F_m^2)}{4R^2 + F_n^2 + F_m^2}\right). \tag{6}$$

Let us consider the special Fibonacci points $P_n(F_n, 0)$ on the x-axis, whose first coordinates are Fibonacci numbers, i.e., $P_0(0, 0), P_{1,2}(1, 0), P_3(2, 0), \ldots, P_n(F_n, 0)$, as shown in Fig. 2(a). The notation $P_{1,2}(1, 0)$ is preferred because $F_1 = F_2$ from (1), which implies that $P_1(1, 0)$ and $P_2(1, 0)$ represent the same point. Let us now try to find coordinate-wise relations between the sequential points $P^{\mathrm{F}}_n(\xi^{\mathrm{F}}_n, \eta^{\mathrm{F}}_n, \zeta^{\mathrm{F}}_n)$, which are the ISP images of the

R	$\lambda_n = -1$	$\lambda_n = +1$
$R = 1/2$	$n < 2$	$n > 2$
$R = 2/2$	$n < 3$	$n > 3$
$R = 3/2$	$n < 4$	$n > 4$
$R = 5/2$	$n < 5$	$n > 5$
$R = 8/2$	$n < 6$	$n > 6$
$R = 13/2$	$n < 7$	$n > 7$
$R = 21/2$	$n < 8$	$n > 8$
$\vdots$	$\vdots$	$\vdots$
$R = F_N/2$	$n < N$	$n > N$

TABLE 1. The dependence of the value of the λ_n's to given Fibonacci point on the x and radius of the sphere.

special Fibonacci points $P_n(F_n, 0)$. The coordinates of the ISP of the points $P_n(F_n, 0)$ are obtained as

$$P^{\mathrm{s}}\left(\xi_n^{\mathrm{F}}, \eta_n^{\mathrm{F}}, \zeta_n^{\mathrm{F}}\right) = P^{\mathrm{s}}\left(\frac{4R^2F_n}{4R^2+F_n^2}, 0, \frac{2RF_n^2}{4R^2+F_n^2}\right).$$

In order to find a relation for the ξ_n^{F}, one can consider the first coordinates and rearrange them as

$$\xi_n^{\mathrm{F}} F_n^2 - 4R^2F_n + 4R^2\xi_n^{\mathrm{F}} = 0$$

which allows us to find

$$F_n = \frac{2R^2 + 2R\lambda_n\sqrt{R^2 - (\xi_n^{\mathrm{F}})^2}}{\xi_n^{\mathrm{F}}}, \tag{7}$$

where λ_n simply equals to ± 1 depending on the values of n and R. Table 1 shows how the radius R and number n determine the sign of $\lambda_n(R)$. As seen from the table, if $R = F_N/2$ for some $N \in \mathbb{N}$ with $N \geq 2$, then $\lambda_n(R)$ is given by

$$\lambda_n(R) = \begin{cases} -1, & n < N \\ +1, & n > N. \end{cases}$$

When $n = N$, $R = \xi_n^{\mathrm{F}}$, the square root in the numerator of (7) becomes zero, and the effect of λ_n in the equation also disappears. If $\frac{F_N}{2} < R < \frac{F_{N+1}}{2}$ then the $\lambda_n(R)$ is given by the following relation:

$$\lambda_n(R) = \begin{cases} -1, & n \leq N \\ +1, & n \geq N+1. \end{cases}$$

Considering the Equation (4) together with the definition of $\lambda_n(R)$, one can conclude that the coordinates of the ISP of the sequential points $P_n(F_n, 0)$ satisfy the following "nonlinear addition" relations:

$$\begin{aligned}
\frac{2R^2 + 2\lambda_n R\sqrt{R^2 - (\xi_n^{\mathrm{F}})^2}}{\xi_n^{\mathrm{F}}} &+ \frac{2R^2 + 2\lambda_{n+1} R\sqrt{R^2 - (\xi_{n+1}^{\mathrm{F}})^2}}{\xi_{n+1}^{\mathrm{F}}} \\
&= \frac{2R^2 + 2\lambda_{n+2} R\sqrt{R^2 - (\xi_{n+2}^{\mathrm{F}})^2}}{\xi_{n+2}^{\mathrm{F}}}, \qquad (8) \\
\eta_n^{\mathrm{F}} = \eta_{n+1}^{\mathrm{F}} = \eta_{n+2}^{\mathrm{F}} &= 0, \qquad (9) \\
\sqrt{\frac{\zeta_n^{\mathrm{F}}}{2R - \zeta_n^{\mathrm{F}}}} + \sqrt{\frac{\zeta_{n+1}^{\mathrm{F}}}{2R - \zeta_{n+1}^{\mathrm{F}}}} &= \sqrt{\frac{\zeta_{n+2}^{\mathrm{F}}}{2R - \zeta_{n+2}^{\mathrm{F}}}}, \qquad (10)
\end{aligned}$$

where short hand notation $\lambda_n = \lambda_n(R)$ is used and they are equal to ± 1 for any n.

Each of the equations (8)-(10) describes a relation for a single coordinate of the sequential points, which are the ISP of Fibonacci points on the x-axis. Using the relation (3), one can find relations for the mixed coordinates of the sequential points on the sphere as

$$\frac{2R\,\xi_n^{\mathrm{F}}}{2R - \zeta_n^{\mathrm{F}}} + \frac{2R\,\xi_{n+1}^{\mathrm{F}}}{2R - \zeta_{n+1}^{\mathrm{F}}} = \frac{2R\,\xi_{n+2}^{\mathrm{F}}}{2R - \zeta_{n+2}^{\mathrm{F}}} \qquad (11)$$

which describes the relation between the first and third coordinates of the sequential points on the sphere. In addition, when Equation (11) is used together with Equation (2), it allows one to find the point $P_{n+2}^{\mathrm{s}}(\xi_{n+2}^{\mathrm{F}}, 0, \zeta_{n+2}^{\mathrm{F}})$ whenever the successive points $P_n^{\mathrm{s}}(\xi_n^{\mathrm{F}}, 0, \zeta_n^{\mathrm{F}})$ and $P_{n+1}^{\mathrm{s}}(\xi_{n+1}^{\mathrm{F}}, 0, \zeta_{n+1}^{\mathrm{F}})$ are known. Note that, Equation (11) is in the form of $a_{n+2} = a_{n+1} + a_n$ with initial values $a_0 = 0$, $a_1 = 1$, thus it is nothing but a different representation of the Fibonacci sequence.

Example 2.1. *In order to illustrate the above discussion, let us consider the sequential Fibonacci points on the x-axis: $P_0(0,0)$, $P_{1,2}(1,0)$, $P_3(2,0)$, and $P_4(3,0)$. The ISP of these points onto the sphere with radius $R = 10$ can be found by substituting $(x,y) = (0,0)$, $(1,0)$, $(2,0)$, and $(3,0)$ into (4), which results in $P_2^{\mathrm{s}}(0,0,0)$, $P_2^{\mathrm{s}}(\frac{400}{401}, 0, \frac{20}{401})$, $P_3^{\mathrm{s}}(\frac{200}{101}, 0, \frac{20}{101})$, and $P_4^{\mathrm{s}}(\frac{1200}{409}, 0, \frac{180}{409})$. It can be easily verified that these image points satisfy the recurrence formulas given in (8)-(11).*

After obtaining the ISP of the Fibonacci points on the x-axis, one can determine the ISP of the points obtained from the counter-clockwise rotation of the Fibonacci points on the x-axis, as shown in Fig. 2(b). These points lie on a line passing through the origin and making an angle α with the positive x-axis, where the distance to the origin is a Fibonacci number [18]. If one considers the special Fibonacci points $P_n(F_n, 0)$ and their rotation about the origin by an angle α through the transformation

$$\begin{pmatrix} x' \\ y' \end{pmatrix} = \begin{pmatrix} \cos\alpha & -\sin\alpha \\ \sin\alpha & \cos\alpha \end{pmatrix} \begin{pmatrix} x \\ y \end{pmatrix}, \qquad (12)$$

the resulting points are given by $P_n'(F_n \cos\alpha, F_n \sin\alpha)$, and since the rotation preserves lengths, the distance between the rotated points and the origin is also a Fibonacci number. It is found that the ISP of these rotated points, ${P'}_n^{\mathrm{s}}(\xi_n', \eta_n', \zeta_n')$, satisfies the following

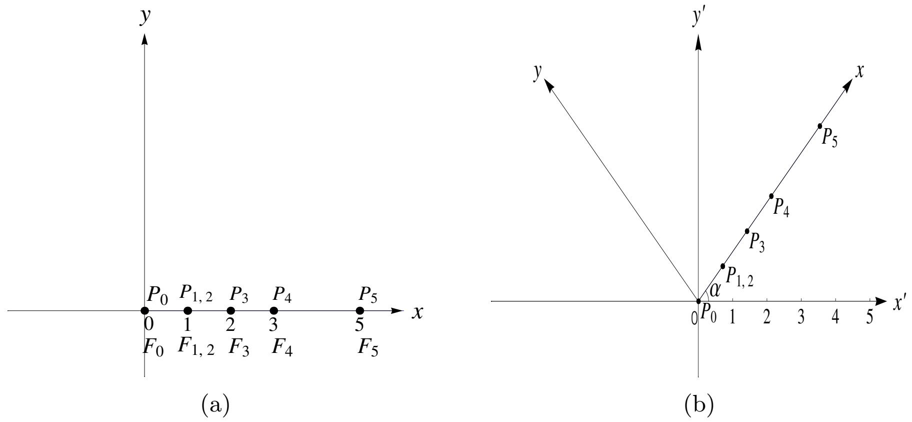

FIGURE 2. (a) Fibonacci points on the x axis. (b) Counter clockwise rotation of Fibonacci points from positive x axis to an oblique line.

relations:

$$\frac{2R^2\cos\alpha + 2\lambda'_n R\sqrt{R^2\cos^2\alpha - (\xi'_n)^2}}{\xi'_n} + \frac{2R^2\cos\alpha + 2\lambda'_{n+1} R\sqrt{R^2\cos^2\alpha - (\xi'_{n+1})^2}}{\xi'_{n+1}}$$
$$= \frac{2R^2\cos\alpha + 2\lambda'_{n+2} R\sqrt{R^2\cos^2\alpha - (\xi'_{n+2})^2}}{\xi'_{n+2}}, \tag{13}$$

$$\frac{2R^2\sin\alpha + 2\lambda'_n R\sqrt{R^2\sin^2\alpha - (\eta'_n)^2}}{\eta'_n} + \frac{2R^2\sin\alpha + 2\lambda'_{n+1} R\sqrt{R^2\sin^2\alpha - (\eta'_{n+1})^2}}{\eta'_{n+1}}$$
$$= \frac{2R^2\sin\alpha + 2\lambda'_{n+2} R\sqrt{R^2\sin^2\alpha - (\eta'_{n+2})^2}}{\eta'_{n+2}}, \tag{14}$$
$$\sqrt{\frac{\zeta'_n}{2R-\zeta'_n}} + \sqrt{\frac{\zeta'_{n+1}}{2R-\zeta'_{n+1}}} = \sqrt{\frac{\zeta'_{n+2}}{2R-\zeta'_{n+2}}}$$

where λ'_ns are equal to ± 1. Their exact values depend on R, n, and α. In (13) and (14), additional $\cos\alpha$ and $\sin\alpha$ terms appear, respectively. For angles α that make these functions positive, $\lambda'_n = \lambda_n$; for angles α that make these functions negative, $\lambda'_n = -\lambda_n$. In the equation (13) when $\cos\alpha = 0$ then $\xi'_n = \xi'_{n+1} = \xi'_{n+2} = 0$. For this case they satisfy $\xi'_{n+2} = \xi'_n + \xi'_{n+1} = 0$, in a similar way the same reasoning is true for the η' in equation (14) when $\sin\alpha = 0$. The relations between the mixed coordinates of the images of the points on the rotated line can also be obtained from Equation (3) as

$$\frac{\xi'_n}{2R-\zeta'_n} + \frac{\xi'_{n+1}}{2R-\zeta'_{n+1}} = \frac{\xi'_{n+2}}{2R-\zeta'_{n+2}}$$
$$\frac{\eta'_n}{2R-\zeta'_n} + \frac{\eta'_{n+1}}{2R-\zeta'_{n+1}} = \frac{\eta'_{n+2}}{2R-\zeta'_{n+2}}. \tag{15}$$

These last two equations, together with the equation (2), allow one to find the point ${P'}^{s}_{n+2}(\xi'_{n+2}, \eta'_{n+2}, \zeta'_{n+2})$ whenever the successive points ${P'}^{s}_{n}(\xi'_{n}, \eta'_{n}, \zeta'_{n})$ and ${P'}^{s}_{n+1}(\xi'_{n+1}, \eta'_{n+1}, \zeta'_{n+1})$ are known.

Example 2.2. *For the rotated version of the Fibonacci points, one can consider the points* $P_2(1,0)$, $P_3(2,0)$ *and* $P_4(3,0)$. *Rotation of these points in the positive direction about the origin with an amount of angle* $\alpha = \pi/3$ *allows us to find rotated points* $P'_2(1/2, \sqrt{3}/2)$, $P'_3(1, \sqrt{3})$ *and* $P'_4(3/2, 3\sqrt{3}/2)$. *ISP of the rotated points onto the sphere with radius* $R = 10$ *can be found by letting* $(x, y) = (1/2, \sqrt{3}/2) = (1, \sqrt{3}) = (3/2, 3\sqrt{3}/2)$ *in equation (4) as* ${P'}^{s}_{2}(\frac{200}{401}, \frac{200\sqrt{3}}{401}, \frac{20}{401})$, ${P'}^{s}_{3}(\frac{100}{101}, \frac{100\sqrt{3}}{101}, \frac{20}{101})$ *and* ${P'}^{s}_{4}(\frac{600}{409}, \frac{600\sqrt{3}}{409}, \frac{180}{409})$.

It can be easily verified that these image points satisfy the recurrence relations (13)-(15). Up to now, only Fibonacci points and their rotations have been considered. However, similar to generalized Fibonacci numbers [7], the concept of Fibonacci points can also be generalized. To achieve this, one may start with the generalized Fibonacci numbers in Equation (1) and follow the described procedure.

2.1. **Fibonacci Identities and Their Transformations.** Fibonacci numbers satisfy a wide variety of identities. In order to illustrate the transformation of the identities, we will consider following relations [19]:

$$F_{n-1}F_{n+1} - F_n^2 = (-1)^n, \tag{16}$$
$$F_{n-1}^2 + F_n^2 = F_{2n-1} \tag{17}$$

which are called the Cassini and Fibonacci square type identities, respectively. Using the Equation (4) and (16), one can find Cassini-type identity for the coordinates of the points on the sphere $P_n^s(\xi_n^F, \eta_n^F, \zeta_n^F)$ which are the ISP of the special Fibonacci points $P_n(F_n, 0)$. Since η's are zero for these special points, one can obtain the Cassini identities related to ξ's and ζ's as

$$\frac{2R^2+2\lambda_{n-1}R\sqrt{R^2-(\xi_{n-1}^F)^2}}{\xi_{n-1}^F} . \frac{2R^2+2\lambda_{n+1}R\sqrt{R^2-(\xi_{n+1}^F)^2}}{\xi_{n+1}^F} - \left(\frac{2R^2+2\lambda_n R\sqrt{R^2-(\xi_n^F)^2}}{\xi_n^F}\right)^2 = (-1)^n$$

and

$$\sqrt{\frac{4R^2\zeta_{n-1}^F}{2R-\zeta_{n-1}^F}} . \sqrt{\frac{4R^2\zeta_{n+1}^F}{2R-\zeta_{n+1}^F}} - \frac{4R^2\zeta_n^F}{2R-\zeta_n^F} = (-1)^n.$$

One can also obtain the other identities for the same special Fibonacci points. For an extension, it is preferred to obtain identities similar to Fibonacci square type identity given in (17) for the rotated special Fibonacci points shown in Fig. 2(b). The Fibonacci square type identities for the coordinates of the image points ${P'}^{s}_{n}(\xi'_n, \eta'_n, \zeta'_n)$ on the sphere are given as follows:

$$\left(\frac{2R^2\cos\alpha + 2\lambda'_{n-1}R\sqrt{R^2\cos^2\alpha - (\xi'_{n-1})^2}}{\xi'_{n-1}}\right)^2 + \left(\frac{2R^2\cos\alpha + 2\lambda'_{n}R\sqrt{R^2\cos^2\alpha - (\xi'_{n})^2}}{\xi'_{n}}\right)^2$$
$$= \frac{2R^2\cos\alpha + 2\lambda'_{2n-1}R\sqrt{R^2\cos^2\alpha - (\xi'_{2n-1})^2}}{\xi'_{2n-1}},$$
$$\left(\frac{2R^2\sin\alpha + 2\lambda'_{n-1}R\sqrt{R^2\sin^2\alpha - (\eta'_{n-1})^2}}{\eta'_{n-1}}\right)^2 + \left(\frac{2R^2\sin\alpha + 2\lambda'_{n}R\sqrt{R^2\sin^2\alpha - (\eta'_{n})^2}}{\eta'_{n}}\right)^2$$
$$= \frac{2R^2\sin\alpha + 2\lambda'_{2n-1}R\sqrt{R^2\sin^2\alpha - (\eta'_{2n-1})^2}}{\eta'_{2n-1}},$$
$$\frac{4R^2\zeta'_{n-1}}{2R-\zeta'_{n-1}} + \frac{4R^2\zeta'_{n}}{2R-\zeta'_{n}} = \sqrt{\frac{4R^2\zeta'_{2n-1}}{2R-\zeta'_{2n-1}}}. \tag{18}$$

Other Fibonacci identities can be transformed in a similar manner and corresponding identities that are satisfied by the coordinates of the image points on the sphere can be found.

2.2. **Fibonacci Numbers and Complex Plane.** Complex numbers $z = x + iy$ can be associated with the points $P(x, y)$ on the plane by assigning the x and y coordinates to the real and imaginary parts of the complex number, respectively [11]. As a result of this interpretation, the stereographic projection of a given point $P^{\mathrm{s}}(\xi, \eta, \zeta)$ on the sphere (except for the north pole) determines a complex number z on the plane as

$$z = \frac{2R\xi}{2R-\zeta} + i\frac{2R\eta}{2R-\zeta}.$$

The inverse stereographic projection of a point represented by a complex number z is given as [11]

$$P^{\mathrm{s}}(\xi,\eta,\zeta) = P^{\mathrm{s}}\left(\frac{2R^2(z+\bar{z})}{4R^2+|z|^2}, \frac{-2iR^2(z-\bar{z})}{4R^2+|z|^2}, \frac{2R|z|^2}{4R^2+|z|^2}\right).$$

Fibonacci points can be represented in terms of complex numbers [20], [21] as

$$z_{n,m} = c_1F_n + ic_2F_m. \tag{19}$$

ISP of the points that are represented by complex numbers in (19), satisfies Equation (6). In addition to this, Equation (6) implies the following relations:

$$\frac{\xi_{n,m}}{2R-\zeta_{n,m}} + \frac{\xi_{n+1,m}}{2R-\zeta_{n+1,m}} = \frac{\xi_{n+2,m}}{2R-\zeta_{n+2,m}} \tag{20}$$
$$\frac{\eta_{n,m}}{2R-\zeta_{n,m}} + \frac{\eta_{n,m+1}}{2R-\zeta_{n,m+1}} = \frac{\eta_{n,m+2}}{2R-\zeta_{n,m+2}}. \tag{21}$$

Complex Fibonacci numbers satisfy the following recurrence relations:

$$z_{n+2,m} = z_{n+1,m} + z_{n,m} - z_{0,m} \tag{22}$$
$$z_{n,m+2} = z_{n,m+1} + z_{n,m} - z_{n,0} \tag{23}$$
$$z_{n+2,m+2} = z_{n+1,m+1} + z_{n,m}. \tag{24}$$

It can be shown that if the complex numbers satisfy the recurrence relations (22) and (23), then their image points satisfy the recurrence relations (20) and (21), respectively. In addition, for the points satisfying the recurrence relation (24), their image points satisfy both recurrence relations (20) and (21). The advantage of the complex number notation is that it allows a compact form. For example, the rotation of the Fibonacci points discussed previously simply correponds to the multiplication of a complex number z with another complex number $w = e^{i\alpha}$ as $z' = wz$, which yields rotated points that obviously have the same length, $|z'| = |e^{i\alpha}z| = |z|$.

In addition to these, the definition of Fibonacci points given in (5) allows us to divide the two-dimensional plane into grids where each grid line at $x = \pm F_n$ and $y = \pm F_m$ passes through Fibonacci points, as illustrated in Fig. 3(a).

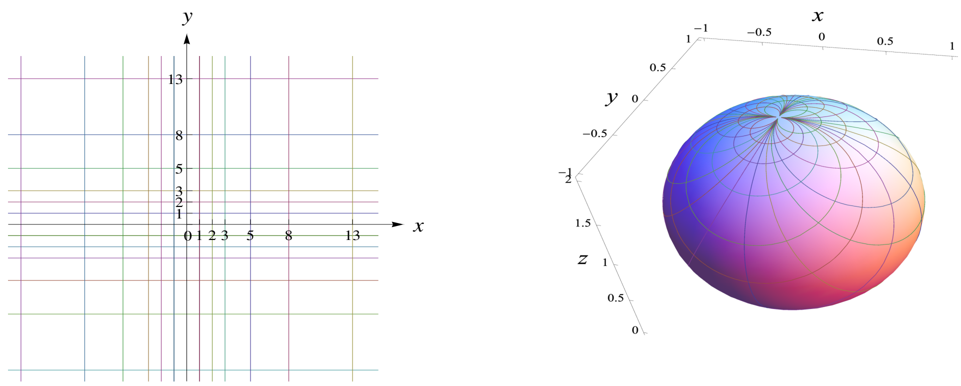

(a) (b)

FIGURE 3. (a) Fibonacci-based grid on the plane. (b) Image of grid the lines on the sphere.

This new style of grid divides the plane into rectangular domains whose boundaries and corners can be expressed in terms of Fibonacci numbers and Fibonacci points, respectively. In Fig. 3(b), the ISP of the grid lines is shown on the unit sphere. The ISP of these rectangular domains forms closed regions with curved boundaries on the sphere, which results in division of the surface of the sphere into curved patches that are directly related to Fibonacci numbers. This new type of division of the surface of the sphere could be interesting in geography for understanding and reinterpreting the surface of the Earth in terms of Fibonacci numbers.

2.3. **Fibonacci Circles and Their Transformations.** Let us consider the circles on the $x-y$ plane whose centers are located at the origin and whose radii are Fibonacci numbers. The equations of these circles can be represented in polar coordinates as $r = F_n$, where r is the standard radial distance in polar coordinates. The parametric representation of these circles can be written in Cartesian coordinates as

$$r_{n,\varphi} = (x_n(\varphi), y_n(\varphi)) = (F_n \cos\varphi, F_n \sin\varphi), \qquad 0 \leq \varphi < 2\pi. \tag{25}$$

ISP of these circles are found to be:

$$r^{\mathrm{s}}_{n,\varphi} = (\xi_n(\varphi), \eta_n(\varphi), \zeta_n(\varphi))$$

where ξ_n, η_n, ζ_n are found by utilizing equations (4) and (25). Since it is known that stereographic projection maps circles to circles [11], the image of the circles in (25) is a set of circles on the sphere whose center is located on the ζ-axis, just above the origin, at a distance of ζ_n and with radius $\xi_n(0)$. These circles and their images on the sphere with radius $R=1$ are shown in Fig. 4(a). In addition to the circles, we consider lines passing through the origin and making an angle with respect to the x-axis that are associated with the Fibonacci numbers as

$$x_n(t)=t\cos(\frac{2\pi W}{F_n}),\qquad y_n(t)=t\sin(\frac{2\pi W}{F_n}),\qquad t\in\mathbb{R}, W\in\mathbb{Z}^+,\ n\neq 0. \tag{26}$$

These lines intersect the Fibonacci circles at the following points:

$$P\left(x(m,n),y(m,n)\right) = \left(F_m\cos(\frac{2\pi W}{F_n}),F_m\sin(\frac{2\pi W}{F_n})\right).$$

The lines and the circles with their images are shown in Fig. 4(b). This figure shows that for geographic applications, the surface of the globe can be divided by Fibonacci related parallels and meridians.

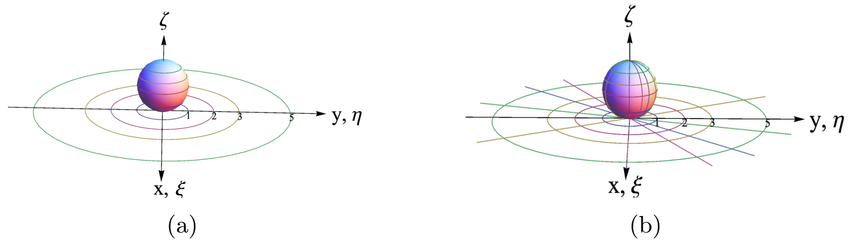

FIGURE 4. (a) Fibonacci circles with Fibonacci number radii $R=1,2,3,5$ and their inverse stereographic projections. (b) Fibonacci circles, lines and their inverse stereographic projections onto the sphere with radius $R=1$. Lines are obtained by taking $n=2,3,4,5,6,7$ and $W=1$ in equation (26).

A simple generalization of the above circles could be the following circles C_n, whose centers are located at the Fibonacci points $P_n(F_n,0)$ and whose radii are Fibonacci numbers F_{n-1}, and they can be described by the following relation:

$$C_n:\qquad (x_n-F_n)^2+y_n^2=F_{n-1}^2,\quad n\in\mathbb{N},\ n\geq 2.$$

Parametric form of these circles is given by

$$x_n(\varphi)=F_n+F_{n-1}\cos\varphi \tag{27}$$

$$y_n(\varphi)=F_{n-1}\sin\varphi \tag{28}$$

where $0\leq\varphi<2\pi$. The ISP of these circles is $C_n^{\mathrm{s}}(\varphi)=(\xi_n(\varphi),\eta_n(\varphi),\zeta_n(\varphi))$ where $\xi_n(\varphi),\eta_n(\varphi),\zeta_n(\varphi)$ are obtained by using $x_n(\varphi)$ and $y_n(\varphi)$ from (27) and (28) in (4). The x coordinates of the intersection points of the Fibonacci circles are described in terms of Fibonacci points as

$$x_n=\begin{cases}\frac{1}{2}\left(\frac{F_{n-1}F_{n+2}-F_{n-2}F_{n+1}}{F_{n-1}}\right), & x_n\in C_n \text{ and } x_n\in C_{n+1}\\ \frac{1}{2}\left(\frac{F_{n+1}F_{n+2}-F_{n-1}F_n}{F_{n+1}}\right), & x_n\in C_n \text{ and } x_n\in C_{n+2}\\ F_{n+1}, & x_n\in C_n \text{ and } x_n\in C_{n+3}.\end{cases} \tag{29}$$

The y coordinates of all intersection points are given by

$$y_n=\pm\sqrt{(F_{n+1}-x_n)(x_n-F_{n-2})}. \tag{30}$$

According to the definition of Fibonacci numbers, it can be shown that there is no intersection point between the circles C_n and C_{n+i} for $i \geq 4$. In addition to this, by (29) and (30), one can deduce that the circles C_n and C_{n+3} always intersect each other at the Fibonacci points on the x axis. Equations (29)–(30) show that the intersection points of the Fibonacci circles can be expressed in terms of Fibonacci numbers.

If the centers of these circles are located on an oblique line passing through the origin, as illustrated in Fig. 2(b), then using (27) and (28) together with (12), one can find their parametric equations and then utilize relation (4) to obtain the ISP of these circles, $C_n^{\mathrm{s}}(\alpha,\varphi) = (\xi_n(\alpha,\varphi), \eta_n(\alpha,\varphi), \zeta_n(\alpha,\varphi))$, where $\xi_n(\alpha,\varphi), \eta_n(\alpha,\varphi), \zeta_n(\alpha,\varphi)$ are obtained by inserting the following expressions into relation (4).

$$\begin{aligned} x_n(\alpha,\varphi) &= (F_n + F_{n-1}\cos\varphi)\cos\alpha - (F_{n-1}\sin\varphi)\sin\alpha \\ y_n(\alpha,\varphi) &= (F_n + F_{n-1}\cos\varphi)\sin\alpha + (F_{n-1}\sin\varphi)\cos\alpha, \quad 0 \leq \varphi, \alpha < 2\pi. \end{aligned}$$

2.4. **Binet-Fibonacci Spiral and Its Inverse Stereographic Projection.** In this subsection ISP of the plane curves is considered. A parametric plane curve can be represented in the form [22]

$$\vec{\gamma}(t) = (x(t), y(t)) \tag{31}$$

where $x(t)$ and $y(t)$ are real-valued continuous functions. The image curve under the inverse stereographic projection is $\vec{\Gamma}^1(t) = (\xi(t), \eta(t), \zeta(t))$, where $\xi(t), \eta(t), \zeta(t)$ are found by substituting $x(t)$ and $y(t)$ from (31) into relation (4). Although ISP can be applied to any parametric curve [23], [24], for the purposes of the present work, we consider the Binet-Fibonacci spiral given by the following parametric equation [25]:

$$\vec{\gamma}^{\,+}(t) = (x(t), y(t)) \;=\; \left(\frac{e^{t\ln\varphi} - \cos\pi t e^{-t\ln\varphi}}{\varphi + \varphi^{-1}}, -\frac{\sin\pi t e^{-t\ln\varphi}}{\varphi + \varphi^{-1}}\right) \tag{32}$$

where $+$ sign indicates that it progresses in the counterclockwise direction. As seen in Fig. 5(a), the intersection points of this curve with the x axis are the Fibonacci points. Image of this curve under the ISP is shown in Fig. 5(b). From the Binet-Fibonacci spiral (32), one can construct a spiral

$$\vec{\gamma}^{\,-}(t) = (x(t), -y(t)) = \left(\frac{e^{t\ln\varphi} - \cos\pi t e^{-t\ln\varphi}}{\varphi + \varphi^{-1}}, \frac{\sin\pi t e^{-t\ln\varphi}}{\varphi + \varphi^{-1}}\right)$$

which progresses in the clockwise direction and passes through Fibonacci points on the x axis. Applying rotation to these spirals with an amount of angle α, one can obtain following spirals

$$\vec{\gamma}^{\,+}(\alpha, t) \;=\; \Big(x(t)\cos(\alpha) - y(t)\sin(\alpha), x(t)\sin(\alpha) + y(t)\cos(\alpha)\Big) \tag{33}$$

$$\vec{\gamma}^{\,-}(\alpha, t) \;=\; \Big(x(t)\cos(\alpha) + y(t)\sin(\alpha), x(t)\sin(\alpha) - y(t)\cos(\alpha)\Big). \tag{34}$$

Using the above definitions, one can rotate spirals by an angle of $\alpha = (2k+1)\pi/2$, $k \in \mathbb{Z}$, which yields rotated spirals passing through the Fibonacci points on the y-axis. Using the Binet-Fibonacci spiral in (32), a deformed spiral can be constructed with the following parametric equation

$$\begin{aligned} x_d(t) &= \frac{e^{t\ln\varphi} - \cos\pi t e^{-t\ln\varphi}}{\varphi + \varphi^{-1}} \\ y_d(t) &= \frac{-\sin\pi t e^{-t\ln\varphi}}{\varphi + \varphi^{-1}} + \beta g(\sin(m\pi t)) \end{aligned} \tag{35}$$

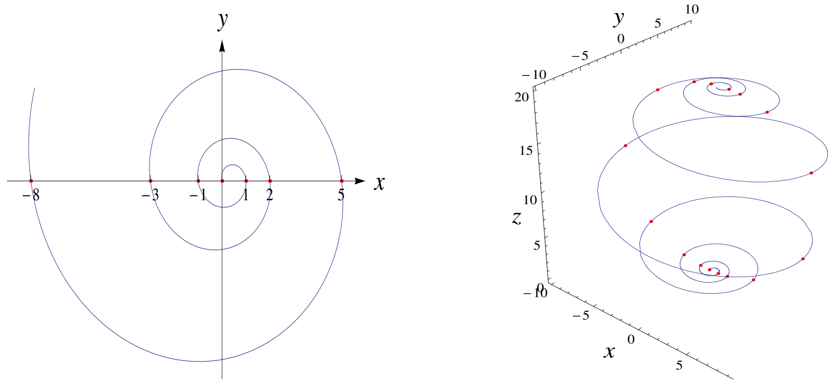

(a) (b)

FIGURE 5. (a) Binet-Fibonacci spiral and Special Fibonacci points $P_n((-1)^{n+1}F_n, 0)$. (b) Inverse stereographic projection of Binet-Fibonacci spiral and Fibonacci points onto the sphere whose center is located at $C(0,0,10)$ and radius $R = 10$. Spiral is obtained for $-2\pi < t < 0$ and for the ISP $-5\pi < t < 0$ is used. For the Fibonacci points $0 \leq n \leq 6$ and $0 \leq n \leq 15$ is used in (a) and (b) respectively.

where g is an arbitrary smooth function, β is a smallness parameter, and m is an arbitrary integer. This new spiral still passes through the Fibonacci points, but its graph has been deformed. The deformed spiral and its ISP onto the sphere are shown in Fig. 6(a) and 6(b), respectively, for $g(x) = x$, $\beta = 0.3$, $m = 20$, and $R = 10$. In addition, replacing $(x(t), y(t))$ in (33) and (34) with $(x_d(t), y_d(t))$ from (35) allows one to obtain both positive and negative winding forms of rotated deformed spirals. These deformed spirals could be useful for describing the environmental effects on plant growth, which cause deviations from perfection.

3. Generalization to the Higher Dimensional Spaces

Stereographic projection can be used in higher dimensional spaces [26]. Let us consider a hyperesphere in $n-$dimensional space

$$X_1^2 + X_2^2 + ... + (X_n - R)^2 = R^2.$$

Stereographic projection of a point $P^{\mathrm{s}} = (X_1, X_2, X_3, \ldots, X_n) \in \mathbb{R}^n$ with respect to the pole $N(0,0,0,\ldots,2R)$ is the point $P(x_1, x_2, x_3, \ldots, x_{n-1}) \in \mathbb{R}^{n-1}$ on the hyperplane such that the relation between them is governed by the following equalities

$$x_k = \frac{2RX_k}{2R - X_n}, \qquad k = 1,2,3,\ldots,n-1$$

and inverse one is

$$X_k = \frac{4R^2 x_k}{\left(\sum\limits_{m=1}^{n-1} x_m^2 + 4R^2\right)}, \qquad k = 1,2,3,\ldots,n-1 \tag{36}$$

$$X_n = \frac{2R\sum\limits_{m=1}^{n-1} x_m^2}{\left(\sum\limits_{m=1}^{n-1} x_m^2 + 4R^2\right)}. \tag{37}$$

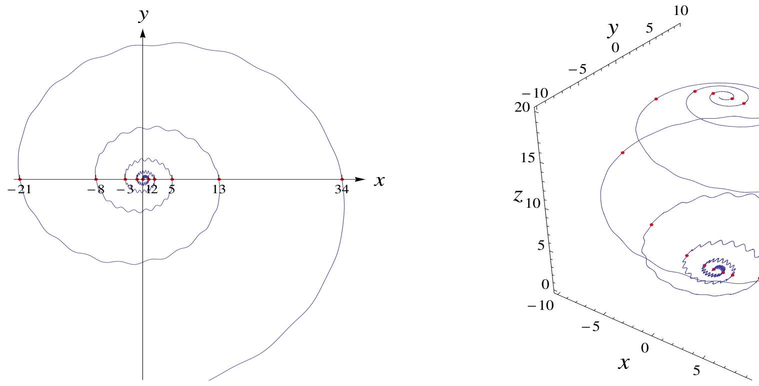

(a) (b)

FIGURE 6. (a) Deformed Binet-Fibonacci spiral and special Fibonacci points $P_n((-1)^{n+1}F_n, 0)$. (b) ISP of that spiral and points onto the sphere whose center is located at $C(0, 0, 10)$ and radius $R = 10$. Deformed plane spiral is obtained for $-3\pi < t < 0$ while its ISP is obtained for $-5\pi < t < 0$. For the Fibonacci points $0 \le n \le 9$ and $0 \le n \le 15$ are used in (a) and (b) respectively.

In order to get a quick insight, let us consider $n = 4$ in equations (36), (37) and take the Fibonacci points $P(F_n, F_m, F_k) \in \mathbb{R}^3$. The inverse stereographic projection of these points with respect to the north pole $N(0, 0, 0, 2R)$ yields the point $P^{\mathrm{s}} = (X_1, X_2, X_3, X_4) \in \mathbb{R}^4$ such that

$$X_1 = \frac{4R^2 F_n}{\left(F_n^2 + F_m^2 + F_k^2 + 4R^2\right)} \tag{38}$$

$$X_2 = \frac{4R^2 F_m}{\left(F_n^2 + F_m^2 + F_k^2 + 4R^2\right)} \tag{39}$$

$$X_3 = \frac{4R^2 F_k}{\left(F_n^2 + F_m^2 + F_k^2 + 4R^2\right)} \tag{40}$$

$$X_4 = \frac{2R(F_n^2 + F_m^2 + F_k^2)}{\left(F_n^2 + F_m^2 + F_k^2 + 4R^2\right)}. \tag{41}$$

One can easily show that the coordinates of the inverse stereographic projection of the special points $P(F_n, F_0, F_0)$, obtained through relations (38)-(41), satisfy recurrence relations similar to those given in equations (8)-(10). Finally, the transformed forms of the Cassini, Fibonacci square type and other related identities can also be found on the hyperspheres by applying the procedures discussed in Section 2.

4. Conclusion

In this study, a novel geometric framework for Fibonacci numbers has been developed by introducing the concept of Fibonacci points and mapping them onto the sphere via inverse stereographic projection (ISP). Through this mapping, nonlinear recurrence relations have been established among the spherical image points, extending the classical Fibonacci relations in a new geometrical context.

The transformation of Fibonacci-related geometrical entities—such as lines, circles, and spirals—onto the sphere has led to the definition of new spherical regions expressed in terms of Fibonacci parallels and meridians. In particular, the introduction of the deformed Binet–Fibonacci spiral, which maintains passage through Fibonacci points while exhibiting controlled deformation, offers a promising model for describing natural deviations observed in biological spirals due to environmental factors. This geometrical interpretation can therefore serve as a mathematical basis for understanding structural irregularities and growth patterns in natural systems. Thus, the findings reveal new links between number theory, geometry, and natural sciences.

Moreover, the present framework suggests potential interdisciplinary applications. Considering the sphere as a Bloch sphere [27], the established relations could be extended to quantum information theory [28], where Fibonacci-structured laser pulses have been shown to enhance information storage in quantum computers [10].

References

[1] Cruz N., Olivares M., Villanueva J., (2017), The golden ratio in Schwarzschild-Kottler black holes, The European Physical Journal C, 77 (2), pp. 1-6.

[2] Pletser V., (2017), Fibonacci numbers and the golden ratio in biology, physics, astrophysics, chemistry and technology: A non-exhaustive review, arXiv preprint, arXiv:1801.01369.

[3] Segerman H., et al., (2010), The sunflower spiral and the Fibonacci metric, Proceedings of Bridges, 20 (10), pp. 483-486.

[4] Hayashi M., Katsu A., Ogiso Y., Takaki, R, (2003), Simulations of sunflower spirals and Fibonacci numbers, Forma-Tokyo, 18 (4), pp. 295-305.

[5] Akhtaruzzaman M., Shafie A. A., (2011), Geometrical substantiation of Phi, the golden ratio and the baroque of nature, architecture, design and engineering, International Journal of Arts, 1 (1), pp. 1-22.

[6] Kustepeli A., Ozbakis B., (2008), The resonant behavior of the Fibonacci fractal tree antennas, Microwave and Optical Technology Letters, 50 (4), pp. 1046-1050.

[7] Horadam A. F., (1961), A generalized Fibonacci sequence, The American Mathematical Monthly, 68 (5), pp. 455-459.

[8] Keskin R., Siar Z., (2013), Some New Identities Concerning Generalized Fibonacci and Lucas Numbers, Hacettepe Journal of Mathematics and Statistics, 42 (3), pp. 211-222.

[9] Aydin F. T., (2018), Dual-complex k-Fibonacci numbers, Chaos, Solitons & Fractals,115, pp. 1-6.

[10] Bohnet J.G., Dumitrescu, P.T., Gaebler, J.P. et al., (2022), Dynamical topological phase realized in a trapped ion quantum simulator, Nature, 607, pp. 63467.

[11] Ahlfors L. V., (1953), Complex analysis: An introduction to the theory of analytic functions of one complex variable, McGraw-Hill.

[12] Silverman R. A., (1984), Complex analysis with applications, Courier Corporation.

[13] Leyshon P. R., Lisle R. J., (2004), Stereographic projection techniques for geologists and civil engineers, Cambridge University Press.

[14] Da Silva L. C., (2021), Holomorphic representation of minimal surfaces in simply isotropic space, Journal of Geometry, 112(3), pp. 35.

[15] Bereta S. J., Caracanhas M. A., Fetter, A. L., (2021). Superfluid vortex dynamics on a spherical film, Physical Review A, 103 (5), pp. 053306.

[16] Aristov D. N., Timofeev V. E., Sorokin A. O., (2019), Towards an effective theory of skyrmion crystals, JETP Letters, 109 (3), pp 207-212.

[17] Mulholland R., Stout D., (1982), Stereographic projection in the national airspace system, IEEE Transactions on Aerospace and Electronic Systems, 1, pp. 48-57.

[18] Arfken G. B., Weber H. J., (2005), Mathematical methods for physicists, Elseiver Inc. .

[19] Koshy T., (2001), Fibonacci and Lucas numbers with applications, John Wiley & Sons, .

[20] Horadam A. F., (1963), Complex Fibonacci numbers and Fibonacci quaternions, The American Mathematical Monthly, 70 (3), pp. 289-291.

[21] Harman C., (1981), Complex Fibonacci numbers, The Fibonacci Quarterly, 19 (1) pp. 82-86.

[22] Dubrovin B., Fomenko A., Novikov S., (2012), Modern geometry: methods and applications,Springer Science & Business Media.

[23] Pashaev O. K., (2014). Two-circles theorem, q-periodic functions and entangled qubit states, J. Phys.: Conf. Ser., 482, pp. 012033.

[24] Parodi B. R., (2020), A generalized Fibonacci spiral, arXiv preprint, arXiv:2004.08902.

[25] Pashaev O.K., Özvatan, M., (2017), Generalized Fibonacci sequences and Binet-Fibonacci curves, arXiv preprint, arXiv:1707.09151.
[26] Karliga B. (1996), On the generalized stereographic projection., Beiträge zur Algebra und Geometrie, 37 (2), pp. 329-336.
[27] Najarbashi G., Seifi B. Mirzaei S. (2016), Two- and three-qubit geometry, quaternionic and octonionic conformal maps, and intertwining stereographic projection, Quantum Inf Process, 15, pp. 509-528.
[28] Siminovitch D. J., (2022), Stereographic projection to and from the Bloch sphere: Visualizing solutions of the Bloch equations and the Bloch-Riccati equation, American Journal of Physics, 90, pp. 755-762.

Barış Ateş has graduated from Department of Mathematics, Marmara University. He hold his M.Sc. and Ph.D. from Izmir Institute of Technology Department of Mathematics. His main research area is Mathematical Physics, especially Electromagnetic wave theory. His research mainly concentrated on the analytical solution of Maxwell equations in deformed spherical regions. He is also interested in Complex Analysis and Number Theory.

Selcan Ateş received her B.Sc. degree in Chemical Engineering from Atatürk University in 2008. She completed her M.Sc. and Ph.D. degrees in Chemical Engineering at İzmir Institute of Technology, earning her Ph.D. in 2018. Her doctoral research focused on the modeling and simulation of the initiated chemical vapor deposition (iCVD) process. Her current research interests include fluid dynamics and hydrometallurgical processes.

Alp Kuştepeli is a professor of Electrical and Electronics Engineering at Izmir Institute of Technology, specializing in computational electromagnetics, microwave engineering, and antenna theory. He received his Ph.D. from Clemson University, USA, in 1999. His research focuses on electromagnetic wave propagation, scattering, and the development of advanced antenna and RF systems.